Precision Measurement of the Branching Fractions of η' Decays

M. Ablikim,[1] M. N. Achasov,[10,d] S. Ahmed,[15] M. Albrecht,[4] M. Alekseev,[55a,55c] A. Amoroso,[55a,55c] F. F. An,[1] Q. An,[52,42] Y. Bai,[41] O. Bakina,[27] R. Baldini Ferroli,[23a] Y. Ban,[35] K. Begzsuren,[25] D. W. Bennett,[22] J. V. Bennett,[5] N. Berger,[26] M. Bertani,[23a] D. Bettoni,[24a] F. Bianchi,[55a,55c] E. Boger,[27,b] I. Boyko,[27] R. A. Briere,[5] H. Cai,[57] X. Cai,[1,42] A. Calcaterra,[23a] G. F. Cao,[1,46] S. A. Cetin,[45b] J. Chai,[55c] J. F. Chang,[1,42] W. L. Chang,[1,46] G. Chelkov,[27,b,c] G. Chen,[1] H. S. Chen,[1,46] J. C. Chen,[1] M. L. Chen,[1,42] P. L. Chen,[53] S. J. Chen,[33] X. R. Chen,[30] Y. B. Chen,[1,42] W. Cheng,[55c] X. K. Chu,[35] G. Cibinetto,[24a] F. Cossio,[55c] H. L. Dai,[1,42] J. P. Dai,[37,h] A. Dbeyssi,[15] D. Dedovich,[27] Z. Y. Deng,[1] A. Denig,[26] I. Denysenko,[27] M. Destefanis,[55a,55c] F. De Mori,[55a,55c] Y. Ding,[31] C. Dong,[34] J. Dong,[1,42] L. Y. Dong,[1,46] M. Y. Dong,[1,42,46] Z. L. Dou,[33] S. X. Du,[60] P. F. Duan,[1] J. Z. Fan,[44] J. Fang,[1,42] S. S. Fang,[1,46] Y. Fang,[1] R. Farinelli,[24a,24b] L. Fava,[55b,55c] F. Feldbauer,[4] G. Felici,[23a] C. Q. Feng,[52,42] M. Fritsch,[4] C. D. Fu,[1] Q. Gao,[1] X. L. Gao,[52,42] Y. Gao,[44] Y. G. Gao,[6] Z. Gao,[52,42] B. Garillon,[26] I. Garzia,[24a] A. Gilman,[49] K. Goetzen,[11] L. Gong,[34] W. X. Gong,[1,42] W. Gradl,[26] M. Greco,[55a,55c] L. M. Gu,[33] M. H. Gu,[1,42] Y. T. Gu,[13] A. Q. Guo,[1] L. B. Guo,[32] R. P. Guo,[1,46] Y. P. Guo,[26] A. Guskov,[27] Z. Haddadi,[29] S. Han,[57] X. Q. Hao,[16] F. A. Harris,[47] K. L. He,[1,46] F. H. Heinsius,[4] T. Held,[4] Y. K. Heng,[1,42,46] Z. L. Hou,[1] H. M. Hu,[1,46] J. F. Hu,[37,h] T. Hu,[1,42,46] Y. Hu,[1] G. S. Huang,[52,42] J. S. Huang,[16] X. T. Huang,[36] X. Z. Huang,[33] Z. L. Huang,[31] T. Hussain,[54] W. Ikegami Andersson,[56] W. Imoehl,[22] M. Irshad,[52,42] Q. Ji,[1] Q. P. Ji,[16] X. B. Ji,[1,46] X. L. Ji,[1,42] H. L. Jiang,[36] X. S. Jiang,[1,42,46] X. Y. Jiang,[34] J. B. Jiao,[36] Z. Jiao,[18] D. P. Jin,[1,42,46] S. Jin,[33] Y. Jin,[48] T. Johansson,[56] N. Kalantar-Nayestanaki,[29] X. S. Kang,[34] M. Kavatsyuk,[29] B. C. Ke,[1] I. K. Keshk,[4] T. Khan,[52,42] A. Khoukaz,[50] P. Kiese,[26] R. Kiuchi,[1] R. Kliemt,[11] L. Koch,[28] O. B. Kolcu,[45b,f] B. Kopf,[4] M. Kuemmel,[4] M. Kuessner,[4] A. Kupsc,[56] M. Kurth,[1] W. Kühn,[28] J. S. Lange,[28] P. Larin,[15] L. Lavezzi,[55c] S. Leiber,[4] H. Leithoff,[26] C. Li,[56] Cheng Li,[52,42] D. M. Li,[60] F. Li,[1,42] F. Y. Li,[35] G. Li,[1] H. B. Li,[1,46] H. J. Li,[1,46] J. C. Li,[1] J. W. Li,[40] K. J. Li,[43] Kang Li,[14] Ke Li,[1] L. K. Li,[1] Lei Li,[3] P. L. Li,[52,42] P. R. Li,[46,7] Q. Y. Li,[36] T. Li,[36] W. D. Li,[1,46] W. G. Li,[1] X. L. Li,[36] X. N. Li,[1,42] X. Q. Li,[34] Z. B. Li,[43] H. Liang,[52,42] Y. F. Liang,[39] Y. T. Liang,[28] G. R. Liao,[12] L. Z. Liao,[1,46] J. Libby,[21] C. X. Lin,[43] D. X. Lin,[15] B. Liu,[37,h] B. J. Liu,[1] C. X. Liu,[1] D. Liu,[52,42] D. Y. Liu,[37,h] F. H. Liu,[38] Fang Liu,[1] Feng Liu,[6] H. B. Liu,[13] H. L. Liu,[41] H. M. Liu,[1,46] Huanhuan Liu,[1] Huihui Liu,[17] J. B. Liu,[52,42] J. Y. Liu,[1,46] K. Y. Liu,[31] Ke Liu,[6] L. D. Liu,[35] Q. Liu,[46] S. B. Liu,[52,42] X. Liu,[30] Y. B. Liu,[34] Z. A. Liu,[1,42,46] Zhiqing Liu,[26] Y. F. Long,[35] X. C. Lou,[1,42,46] H. J. Lu,[18] J. G. Lu,[1,42] Y. Lu,[1] Y. P. Lu,[1,42] C. L. Luo,[32] M. X. Luo,[59] P. W. Luo,[43] T. Luo,[9,j] X. L. Luo,[1,42] S. Lusso,[55c] X. R. Lyu,[46] F. C. Ma,[31] H. L. Ma,[1] L. L. Ma,[36] M. M. Ma,[1,46] Q. M. Ma,[1] X. N. Ma,[34] X. Y. Ma,[1,42] Y. M. Ma,[36] F. E. Maas,[15] M. Maggiora,[55a,55c] S. Maldaner,[26] Q. A. Malik,[54] A. Mangoni,[23b] Y. J. Mao,[35] Z. P. Mao,[1] S. Marcello,[55a,55c] Z. X. Meng,[48] J. G. Messchendorp,[29] G. Mezzadri,[24a] J. Min,[1,42] T. J. Min,[33] R. E. Mitchell,[22] X. H. Mo,[1,42,46] Y. J. Mo,[6] C. Morales Morales,[15] N. Yu. Muchnoi,[10,d] H. Muramatsu,[49] A. Mustafa,[4] S. Nakhoul,[11,g] Y. Nefedov,[27] F. Nerling,[11,g] I. B. Nikolaev,[10,d] Z. Ning,[1,42] S. Nisar,[8] S. L. Niu,[1,42] X. Y. Niu,[1,46] S. L. Olsen,[46] Q. Ouyang,[1,42,46] S. Pacetti,[23b] Y. Pan,[52,42] M. Papenbrock,[56] P. Patteri,[23a] M. Pelizaeus,[4] J. Pellegrino,[55a,55c] H. P. Peng,[52,42] Z. Y. Peng,[13] K. Peters,[11,g] J. Pettersson,[56] J. L. Ping,[32] R. G. Ping,[1,46] A. Pitka,[4] R. Poling,[49] V. Prasad,[52,42] H. R. Qi,[2] M. Qi,[33] T. Y. Qi,[2] S. Qian,[1,42] C. F. Qiao,[46] N. Qin,[57] X. S. Qin,[4] Z. H. Qin,[1,42] J. F. Qiu,[1] S. Q. Qu,[34] K. H. Rashid,[54,i] C. F. Redmer,[26] M. Richter,[4] M. Ripka,[26] A. Rivetti,[55c] M. Rolo,[55c] G. Rong,[1,46] Ch. Rosner,[15] A. Sarantsev,[27,e] M. Savrié,[24b] K. Schoenning,[56] W. Shan,[19] X. Y. Shan,[52,42] M. Shao,[52,42] C. P. Shen,[2] P. X. Shen,[34] X. Y. Shen,[1,46] H. Y. Sheng,[1] X. Shi,[1,42] J. J. Song,[36] W. M. Song,[36] X. Y. Song,[1] S. Sosio,[55a,55c] C. Sowa,[4] S. Spataro,[55a,55c] F. F. Sui,[36] G. X. Sun,[1] J. F. Sun,[16] L. Sun,[57] S. S. Sun,[1,46] X. H. Sun,[1] Y. J. Sun,[52,42] Y. K. Sun,[52,42] Y. Z. Sun,[1] Z. J. Sun,[1,42] Z. T. Sun,[1] Y. T. Tan,[52,42] C. J. Tang,[39] G. Y. Tang,[1] X. Tang,[1] M. Tiemens,[29] B. Tsednee,[25] I. Uman,[45d] B. Wang,[1] B. L. Wang,[46] C. W. Wang,[33] D. Wang,[35] D. Y. Wang,[35] H. H. Wang,[36] K. Wang,[1,42] L. L. Wang,[1] L. S. Wang,[1] M. Wang,[36] Meng Wang,[1,46] P. Wang,[1] P. L. Wang,[1] W. P. Wang,[52,42] X. F. Wang,[1] Y. Wang,[52,42] Y. F. Wang,[1,42,46] Y. Q. Wang,[16] Z. Wang,[1,42] Z. G. Wang,[1,42] Z. Y. Wang,[1] Zongyuan Wang,[1,46] T. Weber,[4] D. H. Wei,[12] P. Weidenkaff,[26] S. P. Wen,[1] U. Wiedner,[4] M. Wolke,[56] L. H. Wu,[1] L. J. Wu,[1,46] Z. Wu,[1,42] L. Xia,[52,42] X. Xia,[36] Y. Xia,[20] D. Xiao,[1] Y. J. Xiao,[1,46] Z. J. Xiao,[32] Y. G. Xie,[1,42] Y. H. Xie,[6] X. A. Xiong,[1,46] Q. L. Xiu,[1,42] G. F. Xu,[1] J. J. Xu,[1,46] L. Xu,[1] Q. J. Xu,[14] X. P. Xu,[40] F. Yan,[53] L. Yan,[55a,55c] W. B. Yan,[52,42] W. C. Yan,[2] Y. H. Yan,[20] H. J. Yang,[37,h] H. X. Yang,[1] L. Yang,[57] R. X. Yang,[52,42] S. L. Yang,[1,46] Y. H. Yang,[33] Y. X. Yang,[12] Yifan Yang,[1,46] Z. Q. Yang,[20] M. Ye,[1,42] M. H. Ye,[7] J. H. Yin,[1] Z. Y. You,[43] B. X. Yu,[1,42,46] C. X. Yu,[34] J. S. Yu,[20] C. Z. Yuan,[1,46] Y. Yuan,[1] A. Yuncu,[45b,a] A. A. Zafar,[54] Y. Zeng,[20] B. X. Zhang,[1] B. Y. Zhang,[1,42] C. C. Zhang,[1] D. H. Zhang,[1] H. H. Zhang,[43] H. Y. Zhang,[1,42] J. Zhang,[1,46] J. L. Zhang,[58] J. Q. Zhang,[4] J. W. Zhang,[1,42,46] J. Y. Zhang,[1] J. Z. Zhang,[1,46] K. Zhang,[1,46] L. Zhang,[44] S. F. Zhang,[33] T. J. Zhang,[37,h] X. Y. Zhang,[36] Y. Zhang,[52,42] Y. H. Zhang,[1,42] Y. T. Zhang,[52,42] Yang Zhang,[1] Yao Zhang,[1] Yu Zhang,[46] Z. H. Zhang,[6]

Z. P. Zhang,[52] Z. Y. Zhang,[57] G. Zhao,[1] J. W. Zhao,[1,42] J. Y. Zhao,[1,46] J. Z. Zhao,[1,42] Lei Zhao,[52,42] Ling Zhao,[1] M. G. Zhao,[34] Q. Zhao,[1] S. J. Zhao,[60] T. C. Zhao,[1] Y. B. Zhao,[1,42] Z. G. Zhao,[52,42] A. Zhemchugov,[27,b] B. Zheng,[53] J. P. Zheng,[1,42] W. J. Zheng,[36] Y. H. Zheng,[46] B. Zhong,[32] L. Zhou,[1,42] Q. Zhou,[1,46] X. Zhou,[57] X. K. Zhou,[52,42] X. R. Zhou,[52,42] X. Y. Zhou,[1] Xiaoyu Zhou,[20] Xu Zhou,[20] A. N. Zhu,[1,46] J. Zhu,[34] J. Zhu,[43] K. Zhu,[1] K. J. Zhu,[1,42,46] S. Zhu,[1] S. H. Zhu,[51] X. L. Zhu,[44] Y. C. Zhu,[52,42] Y. S. Zhu,[1,46] Z. A. Zhu,[1,46] J. Zhuang,[1,42] B. S. Zou,[1] and J. H. Zou[1]

(BESIII Collaboration)

[1]*Institute of High Energy Physics, Beijing 100049, People's Republic of China*
[2]*Beihang University, Beijing 100191, People's Republic of China*
[3]*Beijing Institute of Petrochemical Technology, Beijing 102617, People's Republic of China*
[4]*Bochum Ruhr-University, D-44780 Bochum, Germany*
[5]*Carnegie Mellon University, Pittsburgh, Pennsylvania 15213, USA*
[6]*Central China Normal University, Wuhan 430079, People's Republic of China*
[7]*China Center of Advanced Science and Technology, Beijing 100190, People's Republic of China*
[8]*COMSATS Institute of Information Technology, Lahore, Defence Road, Off Raiwind Road, 54000 Lahore, Pakistan*
[9]*Fudan University, Shanghai 200443, People's Republic of China*
[10]*G.I. Budker Institute of Nuclear Physics SB RAS (BINP), Novosibirsk 630090, Russia*
[11]*GSI Helmholtzcentre for Heavy Ion Research GmbH, D-64291 Darmstadt, Germany*
[12]*Guangxi Normal University, Guilin 541004, People's Republic of China*
[13]*Guangxi University, Nanning 530004, People's Republic of China*
[14]*Hangzhou Normal University, Hangzhou 310036, People's Republic of China*
[15]*Helmholtz Institute Mainz, Johann-Joachim-Becher-Weg 45, D-55099 Mainz, Germany*
[16]*Henan Normal University, Xinxiang 453007, People's Republic of China*
[17]*Henan University of Science and Technology, Luoyang 471003, People's Republic of China*
[18]*Huangshan College, Huangshan 245000, People's Republic of China*
[19]*Hunan Normal University, Changsha 410081, People's Republic of China*
[20]*Hunan University, Changsha 410082, People's Republic of China*
[21]*Indian Institute of Technology Madras, Chennai 600036, India*
[22]*Indiana University, Bloomington, Indiana 47405, USA*
[23a]*INFN Laboratori Nazionali di Frascati, I-00044, Frascati, Italy*
[23b]*INFN and University of Perugia, I-06100, Perugia, Italy*
[24a]*INFN Sezione di Ferrara, I-44122, Ferrara, Italy*
[24b]*University of Ferrara, I-44122, Ferrara, Italy*
[25]*Institute of Physics and Technology, Peace Ave. 54B, Ulaanbaatar 13330, Mongolia*
[26]*Johannes Gutenberg University of Mainz, Johann-Joachim-Becher-Weg 45, D-55099 Mainz, Germany*
[27]*Joint Institute for Nuclear Research, 141980 Dubna, Moscow region, Russia*
[28]*Justus-Liebig-Universitaet Giessen, II. Physikalisches Institut, Heinrich-Buff-Ring 16, D-35392 Giessen, Germany*
[29]*KVI-CART, University of Groningen, NL-9747 AA Groningen, Netherlands*
[30]*Lanzhou University, Lanzhou 730000, People's Republic of China*
[31]*Liaoning University, Shenyang 110036, People's Republic of China*
[32]*Nanjing Normal University, Nanjing 210023, People's Republic of China*
[33]*Nanjing University, Nanjing 210093, People's Republic of China*
[34]*Nankai University, Tianjin 300071, People's Republic of China*
[35]*Peking University, Beijing 100871, People's Republic of China*
[36]*Shandong University, Jinan 250100, People's Republic of China*
[37]*Shanghai Jiao Tong University, Shanghai 200240, People's Republic of China*
[38]*Shanxi University, Taiyuan 030006, People's Republic of China*
[39]*Sichuan University, Chengdu 610064, People's Republic of China*
[40]*Soochow University, Suzhou 215006, People's Republic of China*
[41]*Southeast University, Nanjing 211100, People's Republic of China*
[42]*State Key Laboratory of Particle Detection and Electronics, Beijing 100049, Hefei 230026, People's Republic of China*
[43]*Sun Yat-Sen University, Guangzhou 510275, People's Republic of China*
[44]*Tsinghua University, Beijing 100084, People's Republic of China*
[45a]*Ankara University, 06100 Tandogan, Ankara, Turkey*
[45b]*Istanbul Bilgi University, 34060 Eyup, Istanbul, Turkey*
[45c]*Uludag University, 16059 Bursa, Turkey*
[45d]*Near East University, Nicosia, North Cyprus, Mersin 10, Turkey*
[46]*University of Chinese Academy of Sciences, Beijing 100049, People's Republic of China*

[47]University of Hawaii, Honolulu, Hawaii 96822, USA
[48]University of Jinan, Jinan 250022, People's Republic of China
[49]University of Minnesota, Minneapolis, Minnesota 55455, USA
[50]University of Muenster, Wilhelm-Klemm-Str. 9, 48149 Muenster, Germany
[51]University of Science and Technology Liaoning, Anshan 114051, People's Republic of China
[52]University of Science and Technology of China, Hefei 230026, People's Republic of China
[53]University of South China, Hengyang 421001, People's Republic of China
[54]University of the Punjab, Lahore-54590, Pakistan
[55a]University of Turin, I-10125, Turin, Italy
[55b]University of Eastern Piedmont, I-15121, Alessandria, Italy
[55c]INFN, I-10125, Turin, Italy
[56]Uppsala University, Box 516, SE-75120 Uppsala, Sweden
[57]Wuhan University, Wuhan 430072, People's Republic of China
[58]Xinyang Normal University, Xinyang 464000, People's Republic of China
[59]Zhejiang University, Hangzhou 310027, People's Republic of China
[60]Zhengzhou University, Zhengzhou 450001, People's Republic of China

(Received 12 February 2019; published 9 April 2019)

Based on a sample of $(1310.6 \pm 7.0) \times 10^6 J/\psi$ events collected with the BESIII detector, we present measurements of J/ψ and η' absolute branching fractions using the process $J/\psi \to \gamma\eta'$. By analyzing events where the radiative photon converts into an e^+e^- pair, the branching fraction for $J/\psi \to \gamma\eta'$ is measured to be $(5.27 \pm 0.03 \pm 0.05) \times 10^{-3}$. The absolute branching fractions of the five dominant decay channels of the η' are then measured for the first time and are determined to be $\mathcal{B}(\eta' \to \gamma\pi^+\pi^-) = (29.90 \pm 0.03 \pm 0.55)\%$, $\mathcal{B}(\eta' \to \eta\pi^+\pi^-) = (41.24 \pm 0.08 \pm 1.24)\%$, $\mathcal{B}(\eta' \to \eta\pi^0\pi^0) = (21.36 \pm 0.10 \pm 0.92)\%$, $\mathcal{B}(\eta' \to \gamma\omega) = (2.489 \pm 0.018 \pm 0.074)\%$, and $\mathcal{B}(\eta' \to \gamma\gamma) = (2.331 \pm 0.012 \pm 0.035)\%$, where the first uncertainties are statistical and the second systematic.

DOI: 10.1103/PhysRevLett.122.142002

Even though the main properties of the η' meson are firmly established and its main decay modes are fairly well known, it still attracts both theoretical and experimental attention due to its special role in understanding low energy quantum chromodynamics (QCD). Decays of the η' meson have inspired the study of a wide variety of physics issues, e.g., $\eta - \eta'$ mixing, the light quark masses, as well as physics beyond the standard model. Hence considerable theoretical effort has been devoted to investigate its decay dynamics and partial decay widths with different approaches [1–6]. However, no absolute branching fractions (BFs) of η' decays have yet been measured due to the difficulty of tagging its inclusive decays. The exclusive BFs of the η' summarized by the Particle Data Group (PDG) [7] are all relative measurements. The two most precise measurements so far are from the BES and CLEO experiments. The BES experiment [8] reported the relative BFs of $\mathcal{B}(\eta' \to \gamma\gamma)/\mathcal{B}(\eta' \to \gamma\pi^+\pi^-)$ and $\mathcal{B}(\eta' \to \eta\pi^+\pi^-)/\mathcal{B}(\eta' \to \gamma\pi^+\pi^-)$, while the CLEO experiment [9] measured the branching fractions of its five decay modes by constraining their sum to be $(99.2 \pm 0.2)\%$. The absolute BF measurement of the five dominant decay modes are also essential in order to improve the precision of the BFs for several η' decays, which are obtained via normalization to the dominant η' decay modes.

In this Letter, we develop an approach to measure the absolute BFs of the exclusive decays of the η' meson using a sample of $(1310.6 \pm 7.0) \times 10^6$ J/ψ events [10] collected with the BESIII detector. The design and performance of the BESIII detector are described in detail in Ref. [11]. Taking advantage of the excellent momentum resolution of charged tracks in the main drift chamber (MDC), photon conversions to e^+e^- pairs provide a unique tool to reconstruct the inclusive photon spectrum from radiative J/ψ decays. Take $J/\psi \to \gamma\eta'$, e.g., Monte Carlo (MC) study indicates that the energy resolution of the radiative photon could be improved by a factor of 3 using the photon conversion events. This enables us to tag the η' inclusive decays and then to measure the absolute BF of $J/\psi \to \gamma\eta'$, using

$$\mathcal{B}(J/\psi \to \gamma\eta') = \frac{N^{\mathrm{obs}}_{J/\psi\to\gamma\eta'}}{N_{J/\psi}\varepsilon f}, \qquad (1)$$

where $N^{\mathrm{obs}}_{J/\psi\to\gamma\eta'}$ is the observed η' yield, ε is the detection efficiency obtained from MC simulation, and $N_{J/\psi}$ is the number of J/ψ events. The photon conversion process is simulated with GEANT4 [12], and f is a correction factor to account for the difference in the photon conversion efficiencies between data and MC simulation.

After the η' inclusive measurement, we present precision measurements of η' decays to $\gamma\pi^+\pi^-$, $\eta\pi^+\pi^-$, $\eta\pi^0\pi^0$, $\gamma\omega$, and $\gamma\gamma$, again using J/ψ decays to $\gamma\eta'$, but with the radiative photon directly detected by the electromagnetic calorimeter (EMC) to improve the statistics. With the help of Eq. (1), the BF for each η' exclusive decay is then calculated using

$$\mathcal{B}(\eta' \to X) = \frac{N^{\text{obs}}_{\eta'\to X}}{\varepsilon_{\eta'\to X}} \frac{\varepsilon}{N^{\text{obs}}_{J/\psi\to\gamma\eta'}} f, \tag{2}$$

where $N^{\text{obs}}_{\eta'\to X}$ is the number of signal events obtained from a fit to data and $\varepsilon_{\eta'\to X}$ is the MC-determined reconstruction efficiency.

For the process $J/\psi \to \gamma\eta'$ where the radiative photon converts to an e^+e^- pair, candidate events are required to have at least two oppositely charged tracks. Each charged track is reconstructed using information from the MDC and is required to have a polar angle in the range $|\cos\theta| < 0.93$ and pass within ± 30 cm of the interaction point along the beam direction. To reconstruct the photon conversions, a photon conversion finder [13] is applied to all combinations of track pairs with opposite charge. The photon conversion point (CP) is reconstructed using the two charged track trajectories in the x-y plane, which is perpendicular to the beam line. The photon conversion length R_{xy} is defined as the distance from the beam line to the CP in the x-y plane. Photon conversion events accumulate at $R_{xy} = 3$ and $R_{xy} = 6$ cm corresponding to the position of the beam pipe and the inner wall of the MDC. The detail studies illustrate that the distributions of R_{xy} for data and MC simulations are consistent with each other, as presented in Ref. [13].

To reduce the large combinatorial background from $\pi^0 \to \gamma\gamma$ decays where one of the photons converts into an e^+e^- pair, the e^+e^- pairs that, when combined with a photon candidate, form a π^0 candidate with an invariant mass within 20 MeV/c^2 of the π^0 mass (corresponding to ± 3 times the mass resolution) are not used in the reconstruction. Candidate events with one photon depositing more than 1.2 GeV in the EMC are rejected to suppress background from $e^+e^- \to \gamma\gamma(\gamma)$. A MC study demonstrated that a peaking background contribution is from the electromagnetic Dalitz decay [14] $J/\psi \to \eta' e^+e^-$, which can be effectively removed by requiring $R_{xy} > 2$ cm.

After the above requirements, the recoil mass spectrum of e^+e^-, $M_{\text{recoil}}(e^+e^-)$, is shown in Fig. 1(a), where a clear η' peak is observed with low background. To determine the signal yield of the $J/\psi \to \gamma\eta'$ decays followed by the radiative photon converting into an e^+e^- pair, an unbinned extended maximum likelihood fit to $M_{\text{recoil}}(e^+e^-)$ is performed. The probability density function (PDF) used in the fit consists of three components to describe the mass

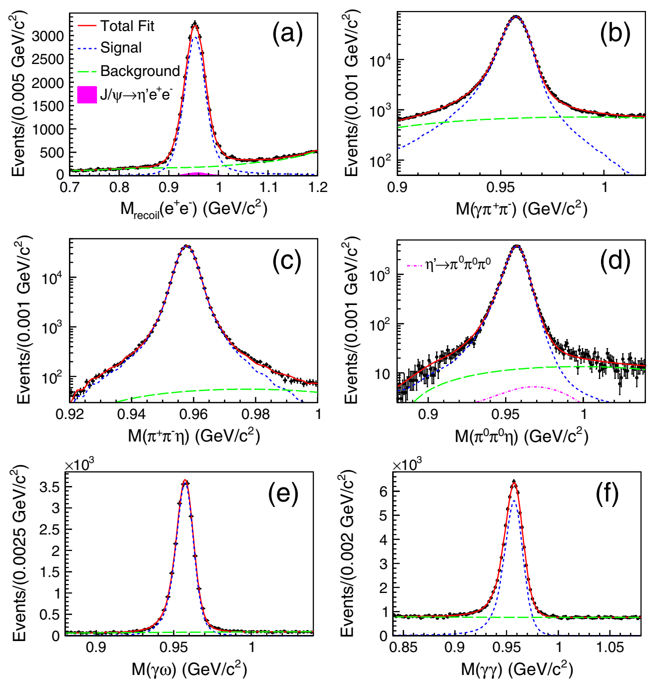

FIG. 1. Unbinned maximum likelihood fit to the invariant mass spectra. The red solid curve shows the result of the fits, the blue dashed line represents the contribution of the signal, and the green dashed line represents the smooth background. The pink histogram in (a) is the peaking background from $J/\psi \to \eta' e^+e^-$, and the pink dashed line in (d) is the peaking background from $\eta' \to \pi^0\pi^0\pi^0$.

spectrum: signal, peaking background from $J/\psi \to e^+e^-\eta'$, and combinatorial background. The signal component is modeled by a MC simulated shape convolved with a Gaussian function to account for the small difference of the mass resolution between MC simulation and data. The parameters of the Gaussian function are free in the fit. The magnitude and shape of the peaking background are obtained from the MC simulation, while the combinatorial background is modeled as the sum of the background shape obtained from an inclusive MC sample of 1.2×10^9 J/ψ events, which is generated with the LUNDCHARM and EVTGEN models [15–17], and a second-order Chebychev polynomial function, which accounts for the difference between inclusive MC sample and data. The fit shown in Fig. 1(a) yields 35980 ± 234 $J/\psi \to \gamma\eta'$ events with the radiative photon converting into an e^+e^- pair.

A MC sample of $J/\psi \to \gamma\eta'$ in which the η' inclusive decays are generated in accordance with the world average BFs of the established modes. We model $\eta' \to \pi^+\pi^-\eta$ and $\eta' \to 3\pi$ according to the distributions measured in Refs. [18,19]; the events of $\eta' \to \gamma\pi^+\pi^-$, $\pi^+\pi^-e^+e^-$, $\pi^+\pi^-\pi^0\pi^0$, and $\pi^+\pi^-\pi^+\pi^-$ are simulated in accordance with theoretical models [20–23], which have been validated in the previous measurements [24–26]; the others, e.g., $\eta' \to \gamma\gamma$ and $\eta' \to \gamma\omega$, are generated with the phase space distribution. Then the detection efficiency is determined to be 5.15×10^{-3} according to the MC simulation. Using this efficiency, we obtained a BF of $J/\psi\to\gamma\eta'$ of $(5.27\pm0.03)\times10^{-3}$ in which we only present the statistical uncertainty. Moreover, we applied a correction factor $f=\varepsilon_{\rm conv}^{\rm data}/\varepsilon_{\rm conv}^{\rm MC}=1.0085\pm0.0050$ [27] to account for the difference in the photon conversion efficiencies.

For the exclusive measurements of η' decays to $\gamma\pi^+\pi^-$, $\eta\pi^+\pi^-$, $\eta\pi^0\pi^0$, $\gamma\omega$, and $\gamma\gamma$ with $\pi^0(\eta)\to\gamma\gamma$ and $\omega\to\pi^+\pi^-\pi^0$, the final states are composed of $\gamma\gamma\pi^+\pi^-$, $\gamma\gamma\gamma\pi^+\pi^-$, $\gamma\gamma\gamma\gamma\gamma\gamma\gamma$, $\gamma\gamma\gamma\gamma\pi^+\pi^-$, and $\gamma\gamma\gamma$, respectively. Candidate events are required to satisfy the following common selection criteria. (i) Candidate charged tracks and photons are selected with the same method as Ref. [28] except that we only use photons hitting the EMC barrel. Since $J/\psi\to\gamma\eta'$ is a two-body decay, the radiative photon from J/ψ decays is monoenergetic with $E=1.4$ GeV, which makes it easy to distinguish the photons from η' decays. The photon with the largest energy is then regarded as the radiative photon from J/ψ. The other photons combined with the charged tracks are used for η' reconstruction. (ii) Events must have the correct number of charged tracks with zero net charge and at least the minimum number of isolated photons associated with the different final states. (iii) The selected events are fitted kinematically. The kinematic fit adjusts the track energy and momentum within the measured uncertainties so as to satisfy energy and momentum conservation for the given event hypothesis. This improves the momentum resolution, selects the correct charged-particle assignment for the tracks, and reduces the background. All possible combinations for each signal mode are tested and the combination with the least χ^2 is retained.

In the case of $\eta'\to\gamma\pi^+\pi^-$, a four-constraint (4C) kinematic fit on the final-state particle candidates is performed and the χ^2_{4C} is required to be less than 100. In order to remove background events with a π^0 in the final states, we require that the invariant mass of $\gamma\gamma$ is not in the π^0 mass region, $|M_{\gamma\gamma}-m_{\pi^0}|>0.02$ GeV$/c^2$, where m_{π^0} is the nominal mass of the π^0 [7]. A MC study of the J/ψ inclusive decays reveals that the channels $J/\psi\to\rho^0\pi^0$ and $J/\psi\to e^+e^-(\gamma)$ are the dominant backgrounds, but neither of them produce peaks in the vicinity of the η' signal in the $\gamma\pi^+\pi^-$ invariant-mass spectrum.

For $\eta'\to\eta\pi^+\pi^-$, a five-constraint (5C) kinematic fit is performed under the $\gamma\gamma\gamma\pi^+\pi^-$ hypothesis with the invariant mass of the two photons being constrained to the η mass [7]. After requiring $\chi^2_{5C}<100$, the remaining data sample contains a very small background level of 0.3%, which is estimated by the events in the η' mass sideband regions. By investigating the J/ψ inclusive MC sample, the dominant background contributions are found to be from $J/\psi\to\gamma\eta\pi^+\pi^-$ and $J/\psi\to\gamma\gamma\rho$, but no peaking background appears in the $\eta\pi^+\pi^-$ invariant mass distribution around the η' signal region.

To detect $\eta'\to\eta\pi^0\pi^0$, one-constraint (1C) kinematic fits are performed on the π^0 (η) candidates reconstructed from photon pairs with the invariant mass of the two photons being constrained to the π^0 (η) mass, and χ^2_{1C} is required to be less than 25. Then a seven-constraint (7C) kinematic fit (two π^0 and one η mass are also constrained in addition to the four energy-momentum constraints) is performed under the hypothesis of $J/\psi\to\gamma\pi^0\pi^0\eta$ and $\chi^2_{7C}<100$ is required. After that the candidate events, as illustrated by the mass spectrum of $\eta\pi^0\pi^0$ in Fig. 1(d), are almost background free. A MC study shows that the background events of $J/\psi\to\gamma\eta'$, $\eta'\to\pi^0\pi^0\pi^0$ contribute to a small peak in the $\eta\pi^0\pi^0$ mass distribution around the η' signal region, which is considered in the signal extraction.

To select $\eta'\to\gamma\omega$ candidates, five-constraint (5C) kinematic fits are performed with the invariant mass of all combinations of any two photons being constrained to the π^0 mass, and χ^2_{5C} is required to be less than 50. We require the $\pi^+\pi^-\pi^0$ invariant mass is in the ω signal region, $|M_{\pi^+\pi^-\pi^0}-m_\omega|<0.03$ GeV$/c^2$, where m_ω is the nominal mass of the ω [7]. If the recoil mass of the ω satisfies $|M_\omega^{\rm rec}-m_{\pi^0}|<0.025\,{\rm GeV}/c^2$ or $|M_\omega^{\rm rec}-m_\eta|<0.035\,{\rm GeV}/c^2$, the events are rejected to suppress background contributions from $J/\psi\to\omega\eta$ and $J/\psi\to\omega\pi^0$. According to a MC study using the J/ψ inclusive sample, the remaining background events mainly come from $J/\psi\to b_1(1235)^0\pi^0$ with $b_1(1235)^0\to\omega\pi^0$ and $J/\psi\to\omega\pi^0\pi^0$, but neither of them produces a peak in the $\gamma\omega$ mass spectrum near the η' mass.

For the decay of $\eta'\to\gamma\gamma$, a 4C-kinematic fit is applied, and events with $\chi^2_{4C}<60$ are selected. Since there is a small probability that the energy of one photon from the η' decay is larger than that of the radiative photon, the mass distributions of the three photon pairs for each event are plotted in Fig. 1(f), where an η' signal is clearly observed above a smooth background due to wrong $\gamma\gamma$ combinations plus other background sources.

After applying the above requirements, the mass spectra of $\gamma\pi^+\pi^-$, $\eta\pi^+\pi^-$, $\eta\pi^0\pi^0$, $\gamma\omega$, and $\gamma\gamma$ are shown in Figs. 1(b)–1(f), where the η' signals for different exclusive decays are clearly observed. The corresponding signal yields are obtained by performing the extended unbinned maximum likelihood fits to the above mass spectra. The PDF function consists of a signal and various background contributions. The signal component is modeled as the MC simulated signal shape convolved with a Gaussian function to account for the difference in the mass resolution between data and MC simulation. The considered background components are subdivided into two classes: (i) the nonpeaking background, which is described with a first-order or second-order Chebychev polynomial function; (ii) the peaking background in $\eta'\to\eta\pi^0\pi^0$, e.g., $J/\psi\to\gamma\eta'$, $\eta'\to\pi^0\pi^0\pi^0$, which is described by the shape determined via a MC simulation and the corresponding

TABLE I. Summary of the measured BFs for η' decays. $N^{\rm obs}_{\eta'\to X}$ is the signal yield from the fits, $\varepsilon_{\eta'\to X}$ is the detection efficiency, and $\mathcal{B}$ is the determined BF.

			$\mathcal{B}(\eta'\to X)(\%)$		$\mathcal{B}/\mathcal{B}(\eta'\to\eta\pi^+\pi^-)$	
Decay mode	$N^{\rm obs}_{\eta'\to X}$	$\varepsilon_{\eta'\to X}(\%)$	This measurement	PDG [7]	This measurement	CLEO [9]
$\eta'\to\gamma\pi^+\pi^-$	$913\,106\pm1052$	44.11	$29.90\pm0.03\pm0.55$	28.9 ± 0.5	$0.725\pm0.002\pm0.010$	$0.677\pm0.024\pm0.011$
$\eta'\to\eta\pi^+\pi^-$	$312\,275\pm570$	27.75	$41.24\pm0.08\pm1.24$	42.6 ± 0.7	…	…
$\eta'\to\eta\pi^0\pi^0$	$51\,680\pm238$	9.08	$21.36\pm0.10\pm0.92$	22.8 ± 0.8	$0.518\pm0.003\pm0.021$	$0.555\pm0.043\pm0.013$
$\eta'\to\gamma\omega$	$22\,749\pm163$	14.98	$2.489\pm0.018\pm0.074$	2.62 ± 0.13	$0.0604\pm0.0005\pm0.0012$	$0.055\pm0.007\pm0.001$
$\eta'\to\gamma\gamma$	$70\,669\pm349$	43.79	$2.331\pm0.012\pm0.035$	2.22 ± 0.08	$0.0565\pm0.0003\pm0.0015$	$0.053\pm0.004\pm0.001$

magnitude is estimated according to the corresponding branching fraction from PDG [7]. The fit results for the signal yields are listed in Table I and the projections of the fit on the mass spectra for different exclusive decays are shown in Figs. 1(b)–1(f), respectively.

According to Eq. (2), the BFs for these five dominant decays of η' are presented in Table I, where the first uncertainties are statistical and the second systematic.

Sources of systematic uncertainties for the BF measurements for η' decays can be divided into two categories: those from the η' exclusive measurements and those from the inclusive measurement.

Systematic uncertainties from the η' exclusive measurements are mainly from the MDC tracking efficiency, the photon detection efficiency, the kinematic fit, and the fit procedure. The MDC tracking efficiency for the charged pion is studied with a control sample of $J/\psi\to\rho\pi$, and the weighted average uncertainties are obtained using bins of transverse momentum [24]. The systematic uncertainty due to the photon detection efficiency is studied with a control sample of $J/\psi\to\pi^+\pi^-\pi^0$ [29]. In $J/\psi\to\gamma\eta'$, the radiative photon carries a unique energy of 1.4 GeV. The detection efficiency of the radiative photon is studied with $J/\psi\to\gamma\eta'$, $\eta'\to\gamma\pi^+\pi^-$. For the uncertainties in the reconstruction of the η and π^0, we use the result of a study described in Ref. [30]. The uncertainty associated with the kinematic fit arises from the inconsistency between the data and the MC simulation. For decay processes including charged tracks in the final states and decay processes with purely neutral particles in the final states, the uncertainties are estimated with helix parameter correction [31] and photon energy correction [32], respectively. The sources of systematic uncertainty in the fit procedures are estimated by varying the fit ranges, background shapes and signal shapes in each fit, uncertainty form peaking background in $\eta'\to\eta\pi^0\pi^0$ is negligible. To estimate the systematic uncertainty due to the kinematics of the η' three-body decays, we generate the $\eta'\to\gamma\pi^+\pi^-$, $\eta'\to\eta\pi^+\pi^-$, and $\eta'\to\eta\pi^0\pi^0$ signal MC samples with parameters from different measurements [18,33,34]. The changes in the reconstruction efficiency are taken as the systematic uncertainties.

In addition to the above exclusive systematic sources, the uncertainty from the η' inclusive measurement is included in the measurement of the BFs. Note that the efficiencies of the electron tracking and the photon conversion reconstruction criteria cancel in the photon conversion efficiency correction. Thus the uncertainties on the η' inclusive measurement consist of uncertainties in the fit procedure, the number of peaking background events from $J/\psi\to e^+e^-\eta'$, the statistical uncertainty on $N^{\rm obs}_{J/\psi\to\gamma\eta'}$ and the uncertainty in the correction factor applied to the photon-conversion efficiency. The total systematic uncertainty from the η' inclusive measurement is 0.9% and it is indicated as the η' inclusive uncertainty in Table II.

In the measurement of the BF for $J/\psi\to\gamma\eta'$, the sources of systematic uncertainty are the same as those for the η' inclusive measurement except that the uncertainty of the number of J/ψ decays [10] is included instead of the statistical uncertainty of $N^{\rm obs}_{J/\psi\to\gamma\eta'}$.

Table II summarizes all contributions to the systematic uncertainties on the BF measurements. In each case, the total systematic uncertainty is given by the quadratic sum of

TABLE II. Summary of all sources of systematic uncertainties (in %) in the η' and J/ψ BF measurements. The ellipses "…" indicate that the uncertainty is not applicable. I–V represent $\eta'\to\gamma\pi^+\pi^-$, $\eta\pi^+\pi^-$, $\eta\pi^0\pi^0$, $\gamma\omega$, and $\gamma\gamma$, respectively, while VI represents $J/\psi\to\gamma\eta'$.

Sources	I	II	III	IV	V	VI
Tracking	1.3	2.3	…	1.9	…	…
Radiative γ	0.2	0.2	0.2	0.2	0.2	…
γ detection	0.5	1.0	3.0	1.5	1.0	…
π^0 reconstruction	…	…	2.0	1.0	…	…
η reconstruction	…	1.0	1.0	…	…	…
Kinematics fit	0.1	0.1	1.7	0.5	0.5	…
Fit range	0.2	0.2	0.2	0.1	0.2	0.3
Signal shape	0.2	0.1	0.1	0.3	0.1	0.2
Background shape	0.3	0.4	0.1	0.1	0.2	0.2
Peaking background	…	…	…	…	…	0.2
Physical model	0.6	0.7	0.5	…	…	…
BFs	…	0.5	0.5	0.8	…	…
f	…	…	…	…	…	0.5
η' inclusive	0.9	0.9	0.9	0.9	0.9	…
$N_{J/\psi}$	…	…	…	…	…	0.53
Total	1.8	3.0	4.3	3.0	1.5	0.9

TABLE III. Comparison of measured decay widths (keV) with theoretical calculations.

	$\Gamma(\eta' \to \eta\pi^+\pi^-)$	$\Gamma(\eta' \to \eta\pi^0\pi^0)$
Reference [1]	77.7	43.8
Reference [5]	83.6 ± 0.8	42.9 ± 0.3
Reference [4]	81 ± 4	46 ± 3
This measurement	80.8 ± 4.4	41.8 ± 2.6

the individual contributions, assuming all sources to be independent.

In summary, using a data sample of $(1310.6 \pm 7.0) \times 10^6 J/\psi$ events collected with the BESIII detector, we present a model-independent measurement of the BF for $J/\psi \to \gamma\eta'$ by analyzing events where the radiative photon converts into an e^+e^- pair. The BF of $J/\psi \to \gamma\eta'$ is determined to be $(5.27 \pm 0.03 \pm 0.05) \times 10^{-3}$, which is in agreement with the world average value [7], but with a significantly improved precision. Taking advantage of the sample of η' inclusive decays tagged by $J/\psi \to \gamma\eta'$ events with photon conversion, the absolute BFs of five dominant decays of the η' are presented in Table I and are measured independently for the first time, which are in agreement with the PDG values [7]. In addition, we give the relative BFs for η' decays as presented in Table I, which are in agreement with CLEO's result [9] within two standard deviations. The precision of our measurements is a factor 2 to 4 better than that of CLEO. The comparisons of the decay widths of $\eta' \to \eta\pi^+\pi^-$ and $\eta' \to \eta\pi^0\pi^0$ with different theoretical approaches, including the chiral unitary approach [1], the chiral perturbation theory [5] and the chiral effective field theory [4], are presented in Table III. Here the measured decay widths are obtained using the η' total decay width $\Gamma(\eta') = 0.196 \pm 0.009$ MeV [7]. Our results are in good agreement with the theoretical estimation. The photon conversion method in this Letter can also be applied in other measurements using J/ψ radiative decays, such as the decay $J/\psi \to \gamma\eta$.

The BESIII Collaboration thanks the staff of BEPCII and the IHEP computing center for their strong support. This work is supported in part by National Key Basic Research Program of China under Contract No. 2015CB856700; National Natural Science Foundation of China (NSFC) under Contracts No. 11335008, No. 11425524, No. 11625523, No. 11635010, No. 11675184, No. 11735014; the Chinese Academy of Sciences (CAS) Large-Scale Scientific Facility Program; the CAS Center for Excellence in Particle Physics (CCEPP); Joint Large-Scale Scientific Facility Funds of the NSFC and CAS under Contracts No. U1532257, No. U1532258, No. U1732263; CAS Key Research Program of Frontier Sciences under Contracts No. QYZDJ-SSW-SLH003, No. QYZDJ-SSW-SLH040; 100 Talents Program of CAS; INPAC and Shanghai Key Laboratory for Particle Physics and Cosmology; Shandong Natural Science Funds for Distinguished Young Scholar under Contract No. JQ201402; German Research Foundation DFG under Contracts No. Collaborative Research Center CRC 1044, No. FOR 2359; Istituto Nazionale di Fisica Nucleare, Italy; Koninklijke Nederlandse Akademie van Wetenschappen (KNAW) under Contract No. 530-4CDP03; Ministry of Development of Turkey under Contract No. DPT2006K-120470; National Science and Technology fund; The Swedish Research Council; U.S. Department of Energy under Contracts No. DE-FG02-05ER41374, No. DE-SC-0010118, No. DE-SC-0010504, No. DE-SC-0012069; University of Groningen (RuG) and the Helmholtzzentrum fuer Schwerionenforschung GmbH (GSI), Darmstadt.

[a]Also at Bogazici University, 34342 Istanbul, Turkey.
[b]Also at the Moscow Institute of Physics and Technology, Moscow 141700, Russia.
[c]Also at the Functional Electronics Laboratory, Tomsk State University, Tomsk, 634050, Russia.
[d]Also at the Novosibirsk State University, Novosibirsk, 630090, Russia.
[e]Also at the NRC "Kurchatov Institute", PNPI, 188300, Gatchina, Russia.
[f]Also at Istanbul Arel University, 34295 Istanbul, Turkey.
[g]Also at Goethe University Frankfurt, 60323 Frankfurt am Main, Germany.
[h]Also at Key Laboratory for Particle Physics, Astrophysics and Cosmology, Ministry of Education; Shanghai Key Laboratory for Particle Physics and Cosmology; Institute of Nuclear and Particle Physics, Shanghai 200240, People's Republic of China.
[i]Also at Government College Women University, Sialkot—51310. Punjab, Pakistan.
[j]Also at Key Laboratory of Nuclear Physics and Ion-beam Application (MOE) and Institute of Modern Physics, Fudan University, Shanghai 200443, People's Republic of China.

[1] N. Beisert and B. Borasoy, Nucl. Phys. **A716**, 186 (2003).
[2] B. Borasoy and R. Nißler, Eur. Phys. J. A **19**, 367 (2004).
[3] B. Borasoy and R Nißler, Nucl. Phys. **A740**, 362 (2004).
[4] B. Borasoy and R. Nißler, Eur. Phys. J. A **26**, 383 (2005).
[5] M. Goodarzi and H. Sadeghi, Int. J. Theor. Phys. **53**, 538 (2014).
[6] A. Faessler, C. Fuchs, and M. I. Krivoruchenko, Phys. Rev. C **61**, 035206 (2000).
[7] M. Tanabashi *et al.* (Particle Data Group), Phys. Rev. D **98**, 030001 (2018).
[8] M. Ablikim *et al.* (BES Collaboration), Phys. Rev. D **73**, 052008 (2006).
[9] T. K. Pedlar *et al.* (CLEO Collaboration), Phys. Rev. D **79**, 111101 (2009).
[10] M. Ablikim *et al.* (BESIII Collaboration), Chin. Phys. C **41**, 013001 (2017).
[11] M. Ablikim *et al.* (BESIII Collaboration), Nucl. Instrum. Methods Phys. Res., Sect. A **614**, 345 (2010).
[12] S. Agostinelli *et al.* (GEANT4 Collaboration), Nucl. Instrum. Methods Phys. Res., Sect. A **506**, 250 (2003).
[13] Z. R. Xu and K. L. He, Chin. Phys. C **36**, 742 (2012).

[14] L. G. Landsberg, Phys. Rep. **128**, 301 (1985).
[15] R. G. Ping, Chin. Phys. C **32**, 599 (2008).
[16] D. J. Lange, Nucl. Instrum. Methods Phys. Res., Sect. A **462**, 152 (2001).
[17] J. C. Chen, G. S. Huang, X. R. Qi, D. H. Zhang, and Y. S. Zhu, Phys. Rev. D **62**, 034003 (2000).
[18] M. Ablikim *et al.* (BESIII Collaboration), Phys. Rev. D **97**, 012003 (2018).
[19] M. Ablikim *et al.* (BESIII Collaboration), Phys. Rev. Lett. **118**, 012001 (2017).
[20] J. Wess and B. Zumino, Phys. Lett. **37B**, 95 (1971).
[21] E. Witten, Nucl. Phys. **B223**, 422 (1983).
[22] T. Petri, arXiv:1010.2378.
[23] F. K. Guo, B. Kubis, and A. Wirzba, Phys. Rev. D **85**, 014014 (2012).
[24] M. Ablikim *et al.* (BESIII Collaboration), Phys. Rev. Lett. **120**, 242003 (2018).
[25] M. Ablikim *et al.* (BESIII Collaboration), Phys. Rev. D **87**, 092011 (2013).
[26] M. Ablikim *et al.* (BESIII Collaboration), Phys. Rev. Lett. **112**, 251801 (2014).
[27] The photon conversion efficiency correction factor is obtained by investigating the photon conversion efficiency in the process $e^+e^- \to \gamma\gamma$ using data samples taken at center-of-mass energies between 2.000 and 3.773 GeV. The photon conversion efficiency is defined as $\varepsilon_{\rm conv} = N_{\rm conv}/(2N_{\gamma\gamma})$, where $N_{\rm conv}$ is the number of observed $e^+e^- \to \gamma\gamma$ events with one converted photon while $N_{\gamma\gamma}$ is the number of observed $e^+e^- \to \gamma\gamma$ events.
[28] M. Ablikim *et al.* (BESIII Collaboration), Phys. Rev. D **96**, 112008 (2017).
[29] M. Ablikim *et al.* (BESIII Collaboration), Phys. Rev. D **92**, 052003 (2015).
[30] M. Ablikim *et al.* (BESIII Collaboration), Phys. Rev. D **81**, 052005 (2010).
[31] M. Ablikim *et al.* (BESIII Collaboration), Phys. Rev. D **87**, 012002 (2013).
[32] M. Ablikim *et al.* (BESIII Collaboration), Phys. Rev. D **94**, 072005 (2016).
[33] V. Dorofeev *et al.*, Phys. Lett. B **651**, 22 (2007).
[34] A. M. Blik *et al.*, Phys. At. Nucl. **72**, 231 (2009).